Padovan,[3] we can transform Eqs. (6) and (16) through the use of the usual finite Fourier exponential transform. Hence

$$\int_0^{2\pi} \{\text{Eqs. (6, 16)}\} e^{-jm\theta} d\theta \rightarrow \tag{17}$$

at $r = r_o, r_i$

$$N_{rrm} + k_1 u_m = \tilde{N}_{rrm} \tag{18a}$$
$$N_m + k_2 v_m = \tilde{N}_m \tag{18b}$$
$$M_{rrm} + k_3 w_{m,r} = \tilde{M}_{rrm} \tag{18c}$$
$$Q_m + k_4 w_m = \tilde{Q}_m \tag{18d}$$

and

$$G_1 \zeta_{m,xxxx} + (G_6 + jmG_2)\zeta_{m,xxx} + (G_{10} - m^2 G_3 + jmG_7)\zeta_{m,xx} + [G_{13} - m^2 G_8 + j(-m^3 G_4 + mG_{11})]\zeta_{m,x} + [G_{15} + m^4 G_5 - m^2 G_{12} + j(-m^3 G_9 + mG_{14})]\zeta + \mathbf{f}_m + \gamma_m{}^*(T_{im}) = \mathbf{0} \tag{19}$$

where $j = (-1)^{1/2}$ and

$$\langle \zeta_m, N_{rrm}, \ldots, \tilde{M}_{rrm}, \mathbf{f}_m, T_{im} \rangle = \frac{1}{2\pi} \int_0^{2\pi} \langle \zeta, N_{rr}, \ldots, \tilde{M}_{rr}, \mathbf{f}, T_i \rangle e^{-jm\theta} d\theta \tag{20}$$

such that

$$\langle \zeta, \ldots \rangle = \sum_{m=-\infty}^{\infty} \langle \zeta_m, \ldots \rangle e^{jm\theta} \tag{21}$$

In spite of its complex form, the homogeneous solution of Eq. (19) can be taken as

$$\zeta_m(x) = \sum_{i=1}^{8} \alpha_{im} \xi_{im} e^{\lambda_{im} x} \tag{22}$$

where the latent roots λ_{im} and their associated latent vectors ξ_{im} must satisfy the following complex polynomial matrix:

$$\{\lambda_{im}{}^4 G_1 + \lambda_{im}{}^3 (G_6 + jmG_2) + \lambda_{im}{}^2 (G_{10} - m^2 G_3 + jmG_7) + \lambda_{im}[G_{13} - m^2 G_8 + j(-m^3 G_4 + mG_{11})] + [G_{15} + m^4 G_5 - m^2 G_{12} + j(-m^3 G_9 + mG_{14})]\}\xi_{im} = \mathbf{0} \tag{23}$$

In particular, λ_{im} must satisfy the complex characteristic polynominal of the pencil of Eq. (23), namely

$$\sum_{i=0}^{8} q_{im} \lambda_{im}{}^{(8-i)} = 0 \tag{24}$$

where q_{im} are complex constants.

The constants α_{im} appearing in Eq. (22) are obtained by satisfying the transformed boundary conditions denoted by Eq. (18). Thus, in terms of Eq. (22), the homogeneous solution of Eqs. (1–6) is given by

$$\begin{Bmatrix} u \\ v \\ w \end{Bmatrix} = \sum_{m=-\infty}^{\infty} \sum_{i=1}^{8} \alpha_{im} \begin{bmatrix} 1 & 0 & 0 \\ 0 & 1 & 0 \\ 0 & 0 & r \end{bmatrix} \xi_{im} r^{\lambda_{im}} e^{jm\theta} \tag{25}$$

Note for the balanced case, Eq. (25) reduces to the solution of Ref. 1.

Numerical Results

To illustrate the substantial effects of laminate configuration as well as local material orientation β (see Fig. 1), the following boundary value problem was chosen

$$r = 7.5 \text{ in., } 36 \text{ in.; } u, v, w, M_\theta \equiv 0$$
$$f_3 = \sigma \cos\theta \quad \text{(lateral pressure)} \tag{26}$$

Since composite shells of revolution are typically spirally wound composites, the plate configuration studied herein will be considered fiber reinforced with logarithmic fiber loci. Figure 1 illustrates the significant effects of fiber orientation on the mechanical fields of a symmetrically and alternately plied four layer plate. The $\beta = 0°$ configuration illustrated can be used as a reference base from which to measure the significant effects of lamination and material anisotropy. It should be noted that for this case $A_{16}, \ldots, D_{26}$ are zero, hence the various mechanical

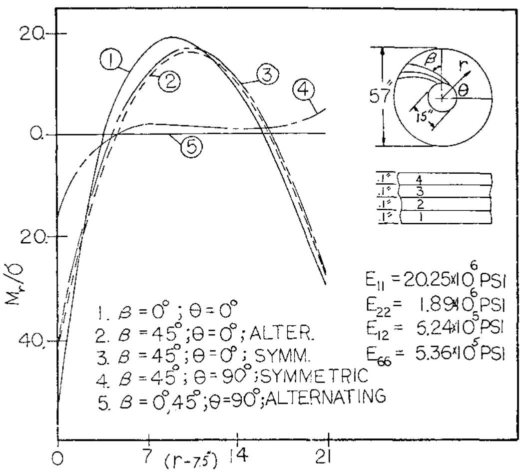

Fig. 1 Effects of β on the M_r field of an alternately and symmetrically plied four-layer simply supported circular plate.

fields are either even or odd. For example, M_r is even, hence $M_r|_{\theta=\pi/2} \equiv 0$.

For the alternately plied configuration, independent of $\beta\varepsilon(0, \pi/2)$, the bending inplane fields are coupled. Furthermore since $A_{16}, \ldots, D_{26}$ are zero, the anisotropic effects of fiber orientation are cancelled. That such is not the case for the symmetrically plied case is clearly seen from the nonzero $M_r|_{\theta=\pi/2}$ field depicted in Fig. 1.

Hence, unlike the alternately plied case, fiber orientation can cause significant asymmetries in the mechanical fields of symmetrically plied laminates. In summary, it should be noted that the analysis given herein can be used to study the effects of laminate configuration and material anisotropy for the generally laminated case.

References

[1] Padovan, J. and Lestingi, J., "Static Solution of Monoclinic Circular Plates," *AIAA Journal*, Vol. 9, No. 12, Dec. 1971, pp. 2473–2475.

[2] Whitney, J. M. and Ashton, J. E., *Theory of Laminated Plates*, Technomic, Stamford, Conn., 1970.

[3] Padovan, J., "Solution of Stresses and Strains for Laminated Monoclinic Cylinders," *AIAA Journal*, Vol. 10, No. 10, Oct. 1972, pp. 1364–1366.

On the Dynamic Buckling of Shells of Revolution

PIN TONG* AND J. ADACHI†

U.S. Army Materials and Mechanics Research Center, Watertown, Mass.

I. Introduction

IN Ref. 1, a series of experiments on the dynamic buckling of thin shallow spherical shells was carried out. The loads on the shell were generated by the rarefaction wave of a shock tube and had very sharp rise times (low μsec). The magnitudes of loading were less than 0.5 psi. The duration of loads on the shell

Received October 5, 1973; revision received January 7, 1974.

Index categories: Structural Dynamic Analysis; Structural Stability Analysis.

* AROD Consultant; also Associate Professor of Aeronautics and Astronautics, MIT, Cambridge, Mass.

† Supervisor Research Mechanical Engineer.

was controllable by varying the length of the shock tube. The purpose of this Note is to examine this series of experiments analytically.

Many authors have examined the dynamic buckling of shells, e.g., see Ref. 2. The governing equations are highly nonlinear and are not amenable to closed form solution. Therefore one must resort to various approximate solutions of this phenomenon. Because of time-dependent nature of the problem, the definition of dynamic buckling itself is not precise and the direct use of the finite-element or finite-different methods can be very costly. In this Note, to reduce the time required for computation, the prebuckling solution and the bifurcation buckling mode are determined by the finite-element method.[3,4] The inertia effect of the prebuckling deformation is ignored. The dynamic responses are studied approximately in terms of amplitudes of the bifurcation modes. Following Budiansky[5] dynamic instability is defined by a large increase of modal amplitude for small increase in load.

II. Mathematical Formulation

The deformation of the shell is assumed in the form

$$\mathbf{u} = \mathbf{u}_o(p) + \mathbf{u}_1\mathbf{A} + \mathbf{u}_2(\mathbf{A}, p) \tag{1}$$

where $\mathbf{u}$ is the displacement vector with its components being (u, v, w), p is the loading magnitude, $\mathbf{u}_o$ is the quasi-static prebuckling deformation $\mathbf{u}_1$ is the bifurcation matrix with its column being the bifurcation modes at the bifurcation load, p_b, $\mathbf{A}$ is the modal amplitude which is time dependent, and $\mathbf{u}_2$ is the quasi-static deformation in terms of $\mathbf{A}$ due to the nonlinear coupling of the prebuckling deformation and various bifurcation modes. For a given loading p, the vectors $\mathbf{u}_o$, $\mathbf{u}_1$, and $\mathbf{u}_2$ are determined in terms of $\mathbf{A}$ by the finite-element method.[3,4] The Hamiltonian Principle for the shell is

$$H = \int_{t_1}^{t_2} [\text{K.E.} - \text{D.E.} - \text{P.E.}]\, dt \tag{2}$$

where K.E., D.E., and P.E. are, respectively, the kinetic, the dissipation, and the potential energies of the shell. In particular, the dissipation energy is written in the form

$$\text{D.E.} = \int (g_s + \rho a)(\partial \mathbf{u}/\partial t)\mathbf{u}\, dS \tag{3}$$

to account for the structural damping, (g_s) and the acoustic damping, (ρ and a are density and sonic velocity of the air).

Using the Hamiltonian Principle, neglecting the inertia due to $\mathbf{u}_o$ and $\mathbf{u}_2$, one can easily derive the equation of motion

$$\mathbf{M}\left(\ddot{\mathbf{A}} + \frac{g_s + \rho a}{\rho_s h}\dot{\mathbf{A}}\right) + \mathbf{K}(p)\mathbf{A} = \mathbf{Q}_I(p)\mu + \mathbf{Q}(\mathbf{A}, p) \tag{4}$$

where ρ_s and h are, respectively, the density and thickness of the shell; $\mathbf{M}$ and $\mathbf{K}$ are, respectively, the mass and the stiffness matrices; $\mathbf{Q}_I$ is the loading vector due to initial imperfection; and $\mathbf{Q}$ is due to nonlinear coupling from the nonlinear strain-displacement relations. It should be noted that if the prebuckling deformation $\mathbf{u}_o$ satisfies the linear equation of the shell, then

$$\mathbf{Q}_I(p) = \mathbf{k}(0) - \mathbf{k}(p) \tag{5}$$

and $\mathbf{Q}$ is independent of p. Equation (4) is solved by direct numerical integration.

a) One-Mode Analysis of Shell of Revolution Subjected to an Axisymmetric Load

The bifurcation occurs at p_b and involves only one circumferential harmonic, say the jth. The dynamic deformation is assumed to be of the form

$$\begin{aligned} u &= U(s,p) + u_o(s) + Au_j^*(s)\cos j\theta + u_{2j}(s)\cos 2j\theta \\ v &= Av_j^*(s)\sin j\theta + v_{2j}(s)\sin 2j\theta \\ w &= W(s,p) + w_o(s) + Aw_j^*(s)\cos j\theta + w_{2j}\cos 2j\theta \end{aligned} \tag{6}$$

in which (s) is the coordinate along the meridian direction; (U, W) are the symmetric prebuckling deformation at load level p; (u_j^*, v_j^*, w_j^*) is the bifurcation mode; and (u_o, w_o) and (u_{2j}, v_{2j}, w_{2j}) are bifurcation deformations due to geometrical nonlinear coupling.

From Eq. (2) we obtain[4]

$$\begin{aligned} H = \int_{t_1}^{t_2} \Big[&\tfrac{1}{2}m\Big(\dot{A}^2 - \underline{\frac{g_s+\rho a}{\rho_s h}\dot{A}A}\Big) - \tfrac{1}{2}k(p)A^2 - \mu Q_I A - \\ &[\tfrac{1}{2}\mathbf{q}_o{}^T\mathbf{K}_o(p)\mathbf{q}_o + \tfrac{1}{2}\mathbf{q}_{2j}{}^T K_{2j}(p)\mathbf{q}_{2j} + \tfrac{1}{2}\mathbf{q}_o{}^T\mathbf{F}_{o,j}A^2 + \\ &\tfrac{1}{2}\mathbf{q}_{2j}{}^T\mathbf{F}_{2j,j}A^2 + \tfrac{1}{2}d_j A^4]\Big] dt \end{aligned} \tag{7}$$

where the term underlined is the dissipation energy, μ is imperfection amplitude of the jth harmonic, and $\mathbf{q}_o$ and $\mathbf{q}_{2j}$ are the nodal value of (u_o, w_o) and (u_{2j}, v_{2j}, w_{2j}) in the finite-element analysis which satisfies the equation[4]

$$\begin{aligned} \mathbf{K}_o(p)\mathbf{q}_o &= -\tfrac{1}{2}\mathbf{F}_{o,j}A^2 \\ K_{2j}(p)\mathbf{q}_{2j} &= -\tfrac{1}{2}\mathbf{F}_{2j,j}A^2 \end{aligned} \tag{8}$$

The Euler equation of Eq. (7) is

$$m\left(\ddot{A} + \frac{g_s+\rho a}{\rho_s h}\dot{A}\right) + k(p)A = Q_I\mu + QA^3 \tag{9}$$

where

$$Q = \tfrac{1}{2}\mathbf{F}_{o,j}{}^T\mathbf{K}_o{}^{-1}(p)\mathbf{F}_{o,j} + \tfrac{1}{2}\mathbf{F}_{2j,j}{}^T\mathbf{K}_{2j}{}^{-1}(p)\mathbf{F}_{2j,j} - 2d_j \tag{10}$$

b) Two-Mode Analysis of Shell of Revolution Subjected to an Axisymmetric Load

If the bifurcations of the jth and $2j$th harmonics occur at the same or nearly the same load level, the dynamic deformation is assumed in the form

$$\begin{aligned} u &= U(s,p) + A_j u_j^*(s)\cos j\theta + A_{2j}u_{2j}^*(s)\cos 2j\theta \\ v &= A_j v_j^*(s)\sin j\theta + A_{2j}v_{2j}^*(s)\sin 2j\theta \\ w &= W(s,p) + A_j w_j^*(s)\cos j\theta + A_{2j}w_{2j}^*(s)\cos 2j\theta \end{aligned} \tag{11}$$

the superscript (*) denotes the bifurcation mode. A substitution of Eq. (11) into Eq. (2) yields

$$\begin{aligned} H = \int_{t_1}^{t_2} \Big[&\tfrac{1}{2}m_j\Big(\dot{A}_j^2 + \underline{\frac{g_s+\rho a}{\rho_s h}\dot{A}_j A_j}\Big) + \\ &\tfrac{1}{2}m_{2j}\Big(\dot{A}_{2j}^2 + \underline{\frac{g_s+\rho a}{\rho_s h}\dot{A}_{2j}A_{2j}}\Big) - \tfrac{1}{2}k_j(p)A_j^2 - \\ &\tfrac{1}{2}k_{2j}(p)A_{2j}^2 + \tfrac{1}{2}cA_j^2 A_{2j}\Big] dt \end{aligned} \tag{12}$$

The Euler equations of Eq. (12) are

$$\begin{aligned} m_j\left(\ddot{A}_j + \frac{g_s+\rho a}{\rho_s h}\dot{A}_j\right) + k_j(p)A_j &= (Q_I)_j\mu_j + cA_jA_{2j} \\ m_{2j}\left(\ddot{A}_{2j} + \frac{g_s+\rho a}{\rho_s h}\dot{A}_j\right) + k_{2j}(p)A_{2j} &= (Q_I)_j\mu_{2j} + \tfrac{1}{2}A_j^2 \end{aligned} \tag{13}$$

c) Local Buckling of Isotropic Spherical Cap

If the buckling wave lengths are small compared to the base dimension of the cap, one may ignore the boundary conditions and use shallow shell equations to describe the bifurcation. In this case the prebuckling solution is simply

$$W = -(1-v)pR^2/2Eh \tag{14}$$

and the bifurcation modes are in the form[6]

$$\begin{aligned} w^* &= \cos\left(k_x\frac{x}{R}\right)\cos\left(k_y\frac{y}{R}\right) \\ f^* &= -\frac{EhR}{q_o{}^2}\cos\left(k_x\frac{x}{R}\right)\cos\left(k_y\frac{y}{R}\right) \end{aligned} \tag{15}$$

for all k_x and k_y satisfying

$$k_x{}^2 + k_y{}^2 = q_o{}^2 \tag{16}$$

and the bifurcation load p_b is given by

$$p_b = \frac{4Eh}{Rq_o{}^2} = \frac{2E}{[3(1-v^2)]^{1/2}}\left(\frac{h}{R}\right)^2 \tag{17}$$

In Eq. (15), f^* is the stress function. Using the same expression as that of Ref. 6 for static analysis, we assume the dynamic deformation of the shell to be in the form

$$w = W + A_1 w_1{}^* + A_2 w_2{}^*$$
$$f = -\tfrac{1}{2}(x^2+y^2)pR + A_1 f_1{}^* + A_2 f_2{}^* \tag{18}$$

where

$$w_1{}^* = h\cos\left(q_o \frac{x}{R}\right)$$
$$f_1{}^* = -ERh^2 q_o{}^{-2}\cos\left(q_o \frac{x}{R}\right)$$
$$w_2{}^* = h\sin\left(\tfrac{1}{2}q_o \frac{x}{R}\right)\sin\left(\frac{(3)^{1/2}}{2} q_o \frac{y}{R}\right) \tag{19}$$
$$f_2{}^* = -ERh^2 q_o{}^{-2}\sin\left(\tfrac{1}{2}q_o \frac{x}{R}\right)\sin\left(\frac{(3)^{1/2}}{2} q_o \frac{y}{R}\right)$$

A substitution of Eq. (18) into Eq. (2), using the appropriate Hamiltonian Functional of shallow shells, gives

$$H = \int_{t_1}^{t_2}\left\{\frac{h^4\rho_s}{4}\left[\dot{A}_1{}^2 + \tfrac{1}{2}\dot{A}_2{}^2 + \frac{g_s+\rho a}{\rho_s h}(\dot{A}_1 A_1 + \tfrac{1}{2}\dot{A}_2 A_2)\right] + \frac{Eh^3}{R}\left[\tfrac{1}{2}\left(1-\frac{p}{p_b}\right)A_1{}^2 - \frac{9c}{32}A_1 A_2{}^2 + \tfrac{1}{4}\left(1-\frac{p}{p_b}\right)A_2{}^2 - \frac{p}{p_b}A_1\mu_1 - \frac{p}{p_b}A_2\mu_2\right\} S\,dt$$

where S is the area of the shell. The Euler equations are

$$\frac{1}{\omega^2}\left[\ddot{A}_1 + \frac{g_s+\rho a}{\rho_s h}A_1\right] + \left(1-\frac{p}{p_b}\right)A_1 = \frac{p}{p_b}u_1 + \frac{9c}{32}A_2{}^2$$
$$\frac{1}{\omega^2}\left[\ddot{A}_2 + \frac{g_s+\rho a}{\rho_s h}A_2\right] + \left(1-\frac{p}{p_b}\right)A_2 = \frac{p}{p_b}\mu_2 + \frac{9c}{8}A_2{}^2 \tag{20}$$

where

$$\omega^2 = (2/R)E/\rho_s$$

III. Numerical Results and Comparison with Experiments

The series of shallow spherical caps tested in Ref. 1 has been examined analytically. The shells were made of clear Vinylite (PVC) with $\rho_s = 0.062$ lb/in.^{3}, $E = 0.475 \times 10^6$ psi, and $\nu = 0.3$, and were clamped at the end of a shock tube. The pressure pulse was generated by rarefaction wave.

In the analysis, the static bifurcation load in its corresponding bifurcation mode and all the quantities defined in Eq. (9) are first determined by the finite-element technique developed in Ref. 4. The imperfection amplitude is estimated from the experimental buckling load of static test. Equation (9) is then solved by direct numerical integration for various pulse magnitudes of 2.2 msec duration. Such a pulse duration is equal to 0.7 to 2.4 periods of the shells considered at $p = 0$. Dynamic instability is defined by the phenomenon that large maximum amplitudes A are produced by small increases in pressure p.

Figure 1 gives the comparison of the one-mode theoretical and the experimental results. It can be seen that the present theory generally gives a lower bound to the experimental data. If the acoustic damping is neglected in the analysis, the theoretical dynamic buckling load will be lower. Computation has also been carried out using local buckling theory for several λ's. The buckling load is generally 10 ~ 20% lower than those given in Fig. 1.

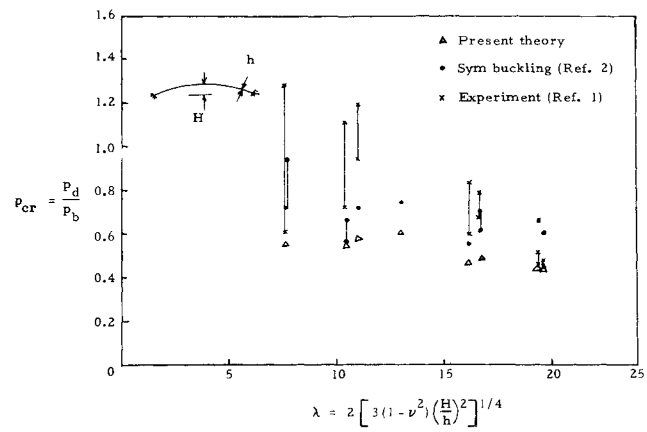

Fig. 1 Dynamic buckling pulse pressure of duration 2.2 m.

References

[1] Adachi, J., Katz, A. H., and Lamothe, R. H., "Response of Shallow Spherical Shells to Pulse Pressure Loads," *Proceedings of the Army Symposium on Solid Mechanics*, Ocean City, Md., Oct. 1972.

[2] Mescall, J. and Tsui, T., "Influence of Damping on Dynamic Stability of Spherical Caps under Step Pressure Loading," *AIAA Journal*, Vol. 9, No. 7, July 1971, pp. 244–248.

[3] Pian, T. H. H. and Tong, P., "Variational Formulation of Finite Displacement Analysis," *High Speed Computing of Elastic Structures (Proceedings of a Symposium of IUTAM)*, edited by M. Fraeijs de Veubeke, University of Liège, Liège, 1971, pp. 43–63.

[4] Tong, P. and Pian, T. H. H., "Postbuckling Analysis of Shells of Revolution by the Finite Element Method," *Thin Shell Structures*, edited by Y. C. Fung and E. E. Sechler, Prentice-Hall, Englewood Cliffs, N.J., 1974, pp. 435–452.

[5] Budiansky, B., "Dynamic Buckling of Elastic Structures," *Dynamics Stability of Structures*, edited by G. Herrmann, Pergamon, Elmsford, N.Y., 1967, pp. 83–106.

[6] Hutchinson, J. W., "Imperfection Sensitivity of Externally Pressured Spherical Shells," *Journal of Applied Mechanics*, Vol. 34, 1967, pp. 49–55.

A Programing Approach to Optimal Structural Design Using Structural Indices

LEONARD SPUNT*
California State University at Northridge, Northridge, Calif.

Introduction

EVER since Michell's classic paper on optimum truss geometry[1] the potential and value of structural efficiency generalizations have been recognized by engineer and theorist alike. Prior to the introduction of the digital computer, investigators employed a parametric approach with algebraic manipulation being the means of appraising relative structural efficiency. Apparently first coined by Wagner,[2] the term "structural index" has played an important role in these parametric approaches. The use of structural indices has historically been associated with the simultaneous mode design technique advanced by Wagner,[2] Farrar,[3] and Shanley[4] and later employed extensively by Gerard[5] and Cox[6] and many other investigators, as can be seen in the recent bibliographies.[7,8] The limitations of simultaneous mode design, which result from the necessary assumptions on the activity of constraints, have led to a recognition that constraints must be expressed as inequalities in the general problem formulation[9] and the attitude that a structural index solution is accordingly forfeit. "Slack variables" have been used recently by the present writer[10] and a similar

Presented as Paper 73-344 at the AIAA/ASME/SAE 14th Structures, Structural Dynamics, and Materials Conference, Williamsburg, Va., March 20–22, 1973; submitted April 10, 1973; revision received December 7, 1973.

Index categories: Aircraft Structural Design (Including Loads); Computer Technology and Computer Simulation Techniques.

* Associate Professor of Engineering. Member AIAA.